ELSEVIER

Physica A 289 (2001) 336–358

PHYSICA A

www.elsevier.com/locate/physa

Non-Newtonian Poiseuille flow of a gas in a pipe

Mohamed Tij[a], Andrés Santos[b,*]

[a] *Département de Physique, Université Moulay Ismaïl, Meknès, Morocco*
[b] *Departamento de Física, Universidad de Extremadura, E-06071 Badajoz, Spain*

Received 12 June 2000

Abstract

The Bhatnagar–Gross–Krook kinetic model of the Boltzmann equation is solved for the steady cylindrical Poiseuille flow fed by a constant gravity field. The solution is obtained as a perturbation expansion in powers of the field (through fourth order) and for a general class of repulsive potentials. The results, which are hardly sensitive to the interaction potential, suggest that the expansion is only asymptotic. A critical comparison with the profiles predicted by the Navier–Stokes equations shows that the latter fail over distances comparable to the mean free path. In particular, while the Navier–Stokes description predicts a monotonically decreasing temperature as one moves apart from the cylinder axis, the kinetic theory description shows that the temperature has a local minimum at the axis and reaches a maximum value at a distance of the order of the mean free path. Within that distance, the radial heat flows from the colder to the hotter points, in contrast to what is expected from the Fourier law. Furthermore, a longitudinal component of the heat flux exists in the absence of gradients along the longitudinal direction. Non-Newtonian effects, such as a non-uniform hydrostatic pressure and normal stress differences, are also present.

PACS: 05.20.Dd; 05.60.−k; 51.10.+y; 47.50.+d

Keywords: Poiseuille flow; Non-Newtonian flow; Kinetic theory; BGK model

1. Introduction

The steady flow in a long channel or in a long tube of circular section under the action of a difference between the pressures imposed at the two ends, usually known as Poiseuille flow or Hagen–Poiseuille flow, is a typical textbook example in fluid dynamics [1–4]. In the last few years, a number of authors [5–15] have analyzed this problem with the channel geometry when the pressure difference is replaced by a

* Corresponding author. Fax: +34-924-289-651.
E-mail address: andres@unex.es (A. Santos).

0378-4371/01/$ - see front matter
PII: S0378-4371(00)00405-2

constant external field **g**. Kadanoff et al. [5,6] have simulated this flow with the FHP lattice gas automaton [16] to confirm the validity of a hydrodynamic description for lattice gas automata. For a dilute gas, Esposito et al. [8] have analyzed the solution of the Boltzmann equation in the Navier–Stokes limit. A generalized Navier–Stokes theory was seen to give a reasonable account of a fluid composed of molecules that possess spin when compared with molecular dynamics simulations [11]. Other studies [7,9,10,12–15], on the other hand, have focused on the breakdown of the continuum hydrodynamic predictions when the strength of the external field is not asymptotically small. In Ref. [7], an exact solution of the Bhatnagar–Gross–Krook (BGK) model kinetic equation was found for a particular value of the field strength. The general solution under the form of an expansion in powers of **g** was considered in Ref. [9], where explicit expressions were derived to fifth order in the field. More recently, the general solution corresponding to the Boltzmann equation for Maxwell molecules has been derived to second order [12] and approximate solutions for hard spheres have been obtained from a Burnett description [14] and by means of moment methods [13,15]. The theoretical predictions of Ref. [9] have been confirmed at a qualitative and semi-quantitative level by numerical simulations of the Boltzmann equation [10,14] and by molecular dynamics simulations [13]. The most surprising of those theoretical predictions is that the temperature profile exhibits a bimodal shape, namely a local minimum at the middle of the channel surrounded by two symmetric maxima at a distance of a few mean free paths. In contrast, the continuum hydrodynamic equations predict a temperature profile with a (flat) maximum at the middle. As a consequence, the Fourier law is dramatically violated since in the slab enclosed by the two maxima the tranverse component of the heat flux is parallel (rather than anti-parallel) to the thermal gradient. Furthermore, non-Newtonian properties, such as normal stress differences and an effective shear viscosity depending on the hydrodynamic gradients, are also present.

The goal of this paper is to carry out a kinetic theory description of the Poiseuille flow driven by an external force when the gas is inside a pipe. The reason is two fold. First, the pipe geometry is much more realistic, and thus more worth studying, than the channel one. Second, it is important to test whether the failure of the continuum description to account for some of the qualitative features of the Poiseuille flow in a channel is not linked to that particular geometry and extends to the pipe case as well. In this context, it is worthwhile noting that an exact solution of the Boltzmann equation (with Maxwell molecules) for the *planar* Fourier flow, which is valid for arbitrary values of the thermal gradient [17,18], does *not* extend to the *cylindrical* geometry [17]. The results reported in this paper, on the other hand, confirm that the structure of the hydrodynamic and flux profiles in the pipe problem is quite similar to that of the channel problem. In particular, the temperature exhibits a non-monotonic behavior as one moves apart from the pipe axis. Nevertheless, the deviations from the continuum description are in general quantitatively smaller than in the channel case.

The paper is organized as follows. The continuum hydrodynamic description is worked out in Section 2, both for the channel and cylindrical geometries. When the

Navier–Stokes constitutive equations are inserted into the exact balance equations for mass, momentum and energy, a closed set of coupled equations for the hydrodynamic fields (pressure, flow velocity and temperature) is obtained. The spatial dependence of the transport coefficients through the temperature is taken into account. Given the nonlinear character of the set of equations, its solution is expressed in powers of the external force. Section 3 is devoted to a summary of the results obtained from the kinetic theory description in the case of the channel Poiseuille flow and a critical comparison with the Navier–Stokes predictions is carried out. The original part of the paper is presented in Section 4, where the BGK kinetic equation is solved for the pipe Poiseuille problem by means of a perturbation expansion in powers of the force. Explicit expressions for the successive contributions to the velocity distribution function through fourth order in the force are derived. By velocity integration, the profiles of the hydrodynamic fields and their fluxes are then obtained. Since the content of Section 4 is rather technical, the discussion of the results is postponed to Section 5, where only terms through third order are considered. As in the planar case, the kinetic theory results strongly differ from the continuum theory expectations, especially in the case of the temperature profile. The breakdown of the Fourier law is characterized by an apparent thermal conductivity coefficient that only for large distances tends to the Navier–Stokes coefficient. Analogously, an apparent shear viscosity coefficient is introduced to monitor deviations from the Newton law. Finally, the main conclusions of the paper are presented in Section 6.

2. Hydrodynamic description

2.1. Channel geometry

Let us first consider the Poiseuille flow in the channel geometry. A fluid is enclosed between two infinite parallel plates normal to the y-axis and located at $y=\pm H$, which are kept at rest. A constant external force per unit mass (e.g., gravity) $\mathbf{g}=g\hat{\mathbf{z}}$ is applied along a direction $\hat{\mathbf{z}}$ parallel to the plates. We assume a laminar and incompressible regime, so in the steady state the physical quantities depend on the coordinate y only. The balance equations for momentum and energy become

$$\frac{\partial P_{yy}}{\partial y}=0\,, \tag{1}$$

$$\frac{\partial P_{yz}}{\partial y}=\rho g\,, \tag{2}$$

$$P_{yz}\frac{\partial u_z}{\partial y}+\frac{\partial q_y}{\partial y}=0\,, \tag{3}$$

where ρ is the mass density, $\mathbf{u}=u_z\hat{\mathbf{z}}$ is the flow velocity, P is the pressure tensor and $\boldsymbol{q}$ is the heat flux. In the Newtonian description these fluxes are related to the

hydrodynamic gradients by the Navier–Stokes (NS) constitutive equations. In this problem they read

$$P_{xx} = P_{yy} = P_{zz} = p\,, \tag{4}$$

$$P_{yz} = -\eta \frac{\partial u_z}{\partial y}\,, \tag{5}$$

$$q_y = -\kappa \frac{\partial T}{\partial y}\,, \tag{6}$$

$$q_z = 0\,, \tag{7}$$

where $p = \frac{1}{3}\mathrm{Tr}\,\mathsf{P}$ is the hydrostatic pressure, T is the temperature, and η and κ are the shear viscosity and the thermal conductivity, respectively. Combining Eqs. (1)–(6), we get

$$\frac{\partial p}{\partial y} = 0\,, \tag{8}$$

$$\frac{\partial}{\partial y}\eta \frac{\partial u_z}{\partial y} = -\rho g\,, \tag{9}$$

$$\frac{\partial}{\partial y}\kappa \frac{\partial T}{\partial y} = -\eta \left(\frac{\partial u_z}{\partial y}\right)^2\,. \tag{10}$$

Eq. (9) gives a parabolic-like velocity profile, that is characteristic of the Poiseuille flow. The temperature profile has, according to Eq. (10), a quartic-like shape. Strictly speaking, these NS profiles are more complicated than just polynomials due to the temperature dependence of the transport coefficients. Since the hydrodynamic profiles must be symmetric with respect to the plane $y = 0$, their odd derivatives must vanish at $y = 0$. Thus, from Eqs. (9) and (10) we have

$$\left.\frac{\partial^2 u_z}{\partial y^2}\right|_{y=0} = -\frac{\rho_0 g}{\eta_0}\,, \tag{11}$$

$$\left.\frac{\partial^2 T}{\partial y^2}\right|_{y=0} = 0\,, \tag{12}$$

$$\left.\frac{\partial^4 T}{\partial y^4}\right|_{y=0} = -2\frac{\rho_0^2 g^2}{\eta_0 \kappa_0}\,, \tag{13}$$

where the subscript 0 denotes quantities evaluated at $y = 0$. According to Eqs. (11)–(13), the NS equations predict that the flow velocity as well as the temperature have a maximum at the middle layer $y = 0$. As we will see in the next Section, the kinetic theory description shows that the temperature actually exhibits a local *minimum* at $y = 0$, since $\partial^2 T/\partial y^2|_{y=0}$ is a positive quantity (of order g^2).

In order to get the hydrodynamic profiles from Eqs. (9) and (10), one needs to know the density and temperature dependence of the transport coefficients. To fix ideas, let

us consider a *dilute* gas of Maxwell molecules, in which case $p \propto \rho T$, $\eta \propto T$, $\kappa \propto T$ [19]. Consequently, from Eqs. (8)–(10) we get

$$p(y) = p_0 \,, \tag{14}$$

$$u_z(y) = u_0 - \frac{\rho_0 g}{2\eta_0}\tilde{y}^{\,2} \,, \tag{15}$$

$$T(y) = T_0 - \frac{\rho_0^2 g^2}{12\eta_0\kappa_0}\tilde{y}^{\,4} \,, \tag{16}$$

where $\tilde{y}$ is an auxiliary space variable defined by $\mathrm{d}\tilde{y} = [T_0/T(y)]\,\mathrm{d}y$. From Eq. (16) the relationship between the true space variable y and the scaled quantity $\tilde{y}$ can be found as

$$y = \tilde{y}\left(1 - \frac{\rho_0^2 g^2}{60\eta_0\kappa_0 T_0}\tilde{y}^{\,4}\right) \,. \tag{17}$$

Eqs. (5) and (6) then imply that

$$P_{yz}(y) = \rho_0 g\tilde{y} \,, \tag{18}$$

$$q_y(y) = \frac{\rho_0^2 g^2}{4\eta_0}\tilde{y}^{\,3} \,. \tag{19}$$

The solution of the fifth-degree equation (17), once inserted into Eqs. (15), (16), (18) and (19), yields the velocity, temperature and flux profiles predicted by the NS equations in the case of Maxwell molecules. To fourth order in the gravity field, the results are

$$u_z(y) = u_0 - \frac{\rho_0 g}{2\eta_0}y^2\left(1 + \frac{\rho_0^2 g^2}{30\eta_0\kappa_0 T_0}y^4\right) + \mathcal{O}(g^5) \,, \tag{20}$$

$$T(y) = T_0 - \frac{\rho_0^2 g^2}{12\eta_0\kappa_0}y^4\left(1 + \frac{\rho_0^2 g^2}{15\eta_0\kappa_0 T_0}y^4\right) + \mathcal{O}(g^6) \,, \tag{21}$$

$$P_{yz}(y) = \rho_0 g y\left(1 + \frac{\rho_0^2 g^2}{60\eta_0\kappa_0 T_0}y^4\right) + \mathcal{O}(g^5) \,, \tag{22}$$

$$q_y(y) = \frac{\rho_0^2 g^2}{3\eta_0}y^3\left(1 + \frac{\rho_0^2 g^2}{20\eta_0\kappa_0 T_0}y^4\right) + \mathcal{O}(g^6) \,. \tag{23}$$

It is interesting to note that $\tilde{y}$ can be eliminated between Eqs. (15) and (16) to obtain the following nonequilibrium "equation of state":

$$T = T_0 - \frac{\eta_0}{3\kappa_0}(u_0 - u_z)^2 \tag{24}$$

which is independent of g. By equation of state we mean in this context a relationship holding locally among the hydrodynamic fields (p, u_z and T) and that is independent of gravity (at least up to a certain order). Since the pressure is uniform in the NS description, it does not enter into Eq. (24). Interestingly enough, a quadratic dependence of the temperature on the flow velocity also appears in the case of the steady planar Couette flow [20].

2.2. Cylindrical geometry

Now we assume that the fluid is inside a straight tube of uniform circular section of radius R. Let the z-axis be parallel to the pipe axis. As before, an external force per unit mass $\mathbf{g} = g\hat{\mathbf{z}}$ is applied to produce a flow field. In the (laminar) steady state all the physically relevant quantities depend only on the distance $r \equiv (x^2 + y^2)^{1/2}$ from the axis. In the case of this cylindrical geometry, the exact balance equations become

$$\frac{\partial}{\partial r}(rP_{rr}) = P_{\phi\phi} \,, \tag{25}$$

$$r^{-1}\frac{\partial}{\partial r}(rP_{rz}) = \rho g \,, \tag{26}$$

$$P_{rz} r\frac{\partial u_z}{\partial r} + \frac{\partial}{\partial r}(rq_r) = 0 \,. \tag{27}$$

These equations constitute the cylindrical counterpart of Eqs. (1)–(3). In general, the relationships between the cylindrical and Cartesian components of a vector $\boldsymbol{A}$ and a tensor B are

$$\begin{pmatrix} A_r \\ A_\phi \\ A_z \end{pmatrix} = \mathsf{U} \cdot \begin{pmatrix} A_x \\ A_y \\ A_z \end{pmatrix} \,, \tag{28}$$

$$\begin{pmatrix} B_{rr} & B_{r\phi} & B_{rz} \\ B_{\phi r} & B_{\phi\phi} & B_{\phi z} \\ B_{zr} & B_{z\phi} & B_{zz} \end{pmatrix} = \mathsf{U} \cdot \begin{pmatrix} B_{xx} & B_{xy} & B_{xz} \\ B_{yx} & B_{yy} & B_{yz} \\ B_{zx} & B_{zy} & B_{zz} \end{pmatrix} \cdot \mathsf{U}^\dagger \,, \tag{29}$$

where

$$\mathsf{U} = \begin{pmatrix} x/r & y/r & 0 \\ -y/r & x/r & 0 \\ 0 & 0 & 1 \end{pmatrix} \tag{30}$$

is a unitary matrix.

The NS constitutive equations yield

$$P_{rr} = P_{\phi\phi} = P_{zz} = p \,, \tag{31}$$

$$P_{rz} = -\eta\frac{\partial u_z}{\partial r} \,, \tag{32}$$

$$q_r = -\kappa\frac{\partial T}{\partial r} \,, \tag{33}$$

$$q_z = 0 \,. \tag{34}$$

The combination of Eqs. (25)–(27), (31)–(33) gives the following hydrodynamic equations:

$$\frac{\partial p}{\partial r} = 0 \,, \tag{35}$$

$$r^{-1}\frac{\partial}{\partial r}\left(r\eta\frac{\partial u_z}{\partial r}\right) = -\rho g\,, \tag{36}$$

$$\frac{\partial}{\partial r}\left(r\kappa\frac{\partial T}{\partial r}\right) = -\eta r\left(\frac{\partial u_z}{\partial r}\right)^2\,. \tag{37}$$

In contrast to what happens in the channel case, Eqs. (8)–(10), it is not possible to obtain the explicit solution to the hydrodynamic equations (35)–(37), even with the help of an auxiliary space variable. On the other hand, the solution can be recursively found as a series expansion in powers of g. To fourth order the result is

$$p(r) = p_0\,, \tag{38}$$

$$u_z(r) = u_0 - \frac{\rho_0 g}{4\eta_0}r^2\left[1 + \frac{(4-3\alpha)\rho_0^2 g^2}{576\eta_0\kappa_0 T_0}r^4\right] + \mathcal{O}(g^5)\,, \tag{39}$$

$$T(r) = T_0 - \frac{\rho_0^2 g^2}{64\eta_0\kappa_0}r^4\left[1 + \frac{(11-9\alpha)\rho_0^2 g^2}{768\eta_0\kappa_0 T_0}r^4\right] + \mathcal{O}(g^6)\,, \tag{40}$$

where we have taken into account that u_z and T must be finite at $r=0$. The subscript 0 now denotes quantities evaluated at $r=0$. Also, we have assumed that $\eta \propto T^{1-\alpha}$, $\kappa \propto T^{1-\alpha}$, which corresponds to repulsive interaction potentials of the form [19] $\varphi(r) \propto r^{-\beta}$ with $\alpha = \frac{1}{2} - 2/\beta$. The cases $\alpha = 0$ and $\alpha = \frac{1}{2}$ correspond to Maxwell molecules ($\beta = 4$) and hard spheres ($\beta \to \infty$), respectively. The corresponding fluxes are

$$P_{rz}(r) = \frac{\rho_0 g}{2}r\left(1 + \frac{\rho_0^2 g^2}{192\eta_0\kappa_0 T_0}r^4\right) + \mathcal{O}(g^5)\,, \tag{41}$$

$$q_r(r) = \frac{\rho_0^2 g^2}{16\eta_0}r^3\left[1 + \frac{(5-3\alpha)\rho_0^2 g^2}{384\eta_0\kappa_0 T_0}r^4\right] + \mathcal{O}(g^6)\,. \tag{42}$$

For arbitrary g the equation of state is not as simple as in the planar case, Eq. (24). Elimination of r between Eqs. (39) and (40) yields

$$T = T_0 - \frac{\eta_0}{4\kappa_0}(u_0 - u_z)^2 - \frac{(1-3\alpha)\eta_0^2}{576\kappa_0^2 T_0}(u_0 - u_z)^4 + \mathcal{O}(g^6)\,. \tag{43}$$

3. Kinetic theory description of the channel Poiseuille flow. A summary

The Poiseuille flow induced by an external force in the channel geometry has been analyzed in the framework of kinetic theory [7,9,12–15], as well as by numerical simulations of the Boltzmann equation [10] and molecular dynamics simulations [13]. The emphasis in these papers, in contrast to that of other works [5,6,8], was put on highlighting the limitations of the NS hydrodynamic description (see Section 2.1) when the strength of the external field g is not small enough.

In this section we briefly summarize the main results derived in Ref. [9] from the BGK model of the Boltzmann equation. The BGK kinetic equation reads [21]

$$\frac{\partial f}{\partial t}+\mathbf{v}\cdot\nabla f+m^{-1}\frac{\partial}{\partial \mathbf{v}}\cdot(\mathbf{F}f)=-\nu(f-f_{\mathrm{LE}}), \tag{44}$$

where $f(\mathbf{r},\mathbf{v},t)$ is the one-particle velocity distribution function, $\mathbf{F}$ is an external force, $\nu(\mathbf{r},t)$ is an effective collision frequency and

$$f_{\mathrm{LE}}(\mathbf{r},\mathbf{v},t)=n(\mathbf{r},t)\left[\frac{m}{2\pi k_B T(\mathbf{r},t)}\right]^{3/2}\exp\left\{-\frac{m[\mathbf{v}-\mathbf{u}(\mathbf{r},t)]^2}{2k_B T(\mathbf{r},t)}\right\} \tag{45}$$

is the local equilibrium distribution function. Here, m is the mass of a particle, k_B is the Boltzmann constant, $n(\mathbf{r},t)$ is the local number density, $\mathbf{u}(\mathbf{r},t)$ is the local flow velocity and $T(\mathbf{r},t)$ is the local temperature. These hydrodynamic fields are defined as velocity moments of f by

$$n=\int d\mathbf{v}\, f, \tag{46}$$

$$n\mathbf{u}=\int d\mathbf{v}\,\mathbf{v} f, \tag{47}$$

$$nk_B T=\frac{m}{3}\int d\mathbf{v}\, V^2 f, \tag{48}$$

where in the last equation we have introduced the peculiar velocity $\mathbf{V}=\mathbf{v}-\mathbf{u}$. The fluxes of momentum and energy are characterized by the pressure tensor

$$P_{ij}=m\int d\mathbf{v}\, V_i V_j f \tag{49}$$

and the heat flux vector

$$\mathbf{q}=\frac{m}{2}\int d\mathbf{v}\, V^2\mathbf{V} f. \tag{50}$$

The trace of the pressure tensor is $3p$, where $p=nk_B T$ is the (local) hydrostatic pressure. The collision frequency ν is proportional to the density and its dependence on the temperature changes in accordance with the interaction potential considered. For instance, $\nu\propto nT^{1/2}$ for hard spheres, while $\nu\propto n$ for Maxwell molecules.

For the steady Poiseuille flow in a channel, the BGK equation (44) reduces to

$$\left(v_y\frac{\partial}{\partial y}+g\frac{\partial}{\partial v_z}\right)f=-\nu(f-f_{\mathrm{LE}}), \tag{51}$$

which must be complemented with the appropriate boundary conditions at $y=\pm H$. On the other hand, we assume that the separation between the plates is large enough to allow for the existence of a *bulk* region $-H+\delta<y<H-\delta$, where δ is the width of the boundary layers and comprises a few mean free paths. Inside the bulk region the solution to Eq. (51) is expected to be rather insensitive to the details of the boundary conditions and depend on y through a functional dependence on the hydrodynamic fields. Such a solution was obtained in Ref. [9] (for Maxwell molecules) by means

of a perturbation expansion in powers of g. Here we quote the hydrodynamic fields through third order

$$p(y) = p_0 \left[1 + \zeta_p \left(\frac{mg}{k_B T_0} \right)^2 y^2 \right] + \mathcal{O}(g^4) , \tag{52}$$

$$u_z(y) = u_0 - \frac{\rho_0 g}{2\eta_0} y^2 \left[1 + \frac{\rho_0^2 g^2}{30\eta_0 \kappa_0 T_0} y^4 + \zeta_u \left(\frac{mg}{k_B T_0} \right)^2 y^2 + \zeta_u' \frac{\rho_0 \eta_0^2 g^2}{p_0^3} \right] + \mathcal{O}(g^5) , \tag{53}$$

$$T(y) = T_0 \left[1 - \frac{\rho_0^2 g^2}{12\eta_0 \kappa_0 T_0} y^4 + \zeta_T \left(\frac{mg}{k_B T_0} \right)^2 y^2 \right] + \mathcal{O}(g^4) , \tag{54}$$

where $\zeta_p = \frac{6}{5} = 1.2$, $\zeta_u = \frac{152}{25} = 6.08$, $\zeta_u' = \frac{5474}{25} = 218.96$, and $\zeta_T = \frac{19}{25} = 0.76$. The BGK predictions (52)–(54) have been confirmed by an exact solution of the Boltzmann equation for Maxwell molecules [12] ($\zeta_p = \frac{6}{5}$, $\zeta_T \simeq 1.0153$), as well as by approximate solutions of the Boltzmann equation for hard spheres by a 13-moment method [13,15] ($\zeta_p = \frac{6}{5}$, $\zeta_T = \frac{14}{25} = 0.56$) and a 19-moment method [15] ($\zeta_p \simeq 1.214$, $\zeta_T \simeq 0.99$). Comparison with the NS predictions, Eqs. (14), (20) and (21), shows that the latter already fail to second order ($\zeta_p^{\rm NS} = \zeta_T^{\rm NS} = 0$) and to third order ($\zeta_u^{\rm NS} = \zeta_u'^{\rm NS} = 0$) in g. According to Eqs. (52)–(54), the pressure increases parabolically from the midpoint ($\zeta_p > 0$) rather than being uniform, the velocity profile has an enhanced quadratic coefficient ($\zeta_u' > 0$) plus a new quartic term ($\zeta_u > 0$), and the temperature has a positive quadratic term ($\zeta_T > 0$). The latter is responsible for the fact that $\partial^2 T/\partial y^2|_{y=0} > 0$, in contrast to the NS prediction (12), so the temperature presents a local *minimum* at $y = 0$ rather than a maximum. This minimum is surrounded by two maxima located at $y = y_{\max} = \pm\sqrt{6\zeta_T}\ell_0$, where $\ell_0 \equiv (\eta_0 \kappa_0 T_0)^{1/2}/p_0$ is a reference mean free path [15]. The relative difference between the maxima and the minimum is $(T_{\max} - T_0)/T_0 = 3\zeta_T^2 (\ell_0/h_0)^2$, where $h_0 \equiv (k_B T_0/m)/g$ is the so-called scale height [22,23], i.e., the characteristic distance associated with the external (gravity) field. This surprising bimodal form of the temperature profile is an effect going beyond the Burnett description [14] and has been confirmed by Monte Carlo simulations of the Boltzmann equation for hard spheres [10,14]. The NS equation of state (24) is now augmented by an extra term

$$T = T_0 - \frac{\eta_0}{3\kappa_0}(u_0 - u_z)^2 + \frac{\zeta_T}{\zeta_p}\frac{T_0}{p_0}(p - p_0) + \mathcal{O}(g^4) . \tag{55}$$

In addition to the hydrodynamic profiles, the momentum and heat fluxes are obtained from the kinetic theory description. In the case of the BGK model, the results are [9]

$$P_{xx}(y) = p_0 \left[1 - \frac{22}{25}\frac{\rho_0 \eta_0^2 g^2}{p_0^3} + \frac{4}{5}\left(\frac{mg}{k_B T_0} \right)^2 y^2 \right] + \mathcal{O}(g^4) , \tag{56}$$

$$P_{yy}(y) = p_0 \left(1 - \frac{306}{25}\frac{\rho_0 \eta_0^2 g^2}{p_0^3} \right) + \mathcal{O}(g^4) , \tag{57}$$

$$P_{zz}(y) = p_0 \left[1 + \frac{328}{25} \frac{\rho_0 \eta_0^2 g^2}{p_0^3} + \frac{14}{5} \left(\frac{mg}{k_B T_0} \right)^2 y^2 \right] + \mathcal{O}(g^4) , \tag{58}$$

$$P_{yz}(y) = \rho_0 g y \left[1 + \frac{\rho_0^2 g^2}{60 \eta_0 \kappa_0 T_0} y^4 + \frac{11}{75} \left(\frac{mg}{k_B T_0} \right)^2 y^2 \right] + \mathcal{O}(g^5) , \tag{59}$$

$$q_y(y) = \frac{\rho_0^2 g^2}{3\eta_0} y^3 + \mathcal{O}(g^4) , \tag{60}$$

$$q_z(y) = -\frac{2mg\kappa_0}{5k_B} \left[1 - \frac{21162 \rho_0 \eta_0^2 g^2}{25 p_0^3} - \frac{159}{5} \left(\frac{mg}{k_B T_0} \right)^2 y^2 - \frac{29 \rho_0^2 g^2}{12 \eta_0 \kappa_0 T_0} y^4 \right] + \mathcal{O}(g^5) . \tag{61}$$

As expected, the fluxes differ from the NS results, Eqs. (4), (7), (22) and (23). The main deviations of the hydrodynamic and flux profiles from the NS predictions occur for distances on the scale of the mean free path, i.e., in the regime where a hydrodynamic description is not expected to hold. For instance, the extra terms appearing in Eq. (53) are, relative to the g^2-term of Eq. (20), of orders $(y/\ell_0)^{-2}$ and $(y/\ell_0)^{-4}$. In addition, the ratio between the component of the heat flux parallel to the flow direction (q_z) and the component parallel to the thermal gradient (q_y) is of order $(y/\ell_0)^{-3}(h_0/\ell_0)$. Thus, the NS description applies in the regime $(y/\ell_0) \gg (h_0/\ell_0)^{1/3} \gg 1$. On the other hand, the kinetic theory description, while limited here to weak fields, i.e., $(h_0/\ell_0) \gg 1$, is still valid for $y \sim \ell_0$.

4. Kinetic theory description of the pipe Poiseuille flow

Now we are going to analyze the solution of the BGK equation for the steady Poiseuille flow problem in a cylindrical geometry. In that case, Eq. (44) becomes

$$\left(v_r \frac{\partial}{\partial r} + \frac{v_\phi}{r} \frac{\partial}{\partial \phi} + g \frac{\partial}{\partial v_z} \right) f = -\nu (f - f_{\mathrm{LE}}) . \tag{62}$$

Note that the derivative $\partial/\partial\phi$ is understood at constant (v_x, v_y), *not* at constant (v_r, v_ϕ). In fact, $\partial v_r/\partial\phi = v_\phi$ and $\partial v_\phi/\partial\phi = -v_r$, and so

$$\frac{\partial f}{\partial \phi} = v_\phi \frac{\partial f}{\partial v_r} - v_r \frac{\partial f}{\partial v_\phi} . \tag{63}$$

The exact conservation equations (25)–(27) can be reobtained from Eq. (62) by multiplying both sides by v_r, v_z and V^2, respectively, and integrating over the velocity.

As in Section 2, we denote by a subscript 0 those quantities evaluated at the axis of the pipe ($r = 0$). Thus, $v_0 \equiv (k_B T_0/m)^{1/2}$ is a thermal velocity, $\lambda_0 \equiv v_0/\nu_0$ is a mean free path and $h_0 \equiv v_0^2/g$ is a characteristic length associated with gravity (scale height). Since in the BGK model $\eta = p/\nu$ and $\kappa = 5k_B\eta/2m$, one has $\ell_0 = \sqrt{\frac{5}{2}}\lambda_0$, where ℓ_0

was introduced in the previous Section. Without loss of generality, we will assume a reference frame stationary with the flow at $r = 0$, so $u_0 = 0$. We next introduce dimensionless quantities as

$$\mathbf{v}^* = v_0^{-1}\mathbf{v}, \qquad \mathbf{r}^* = \lambda_0^{-1}\mathbf{r}, \qquad f^* = n_0^{-1}v_0^3 f\,, \tag{64}$$

$$p^* = p_0^{-1}\,p, \qquad \mathbf{u}^* = v_0^{-1}\mathbf{u}, \qquad T^* = T_0^{-1}T\,, \tag{65}$$

$$v^* = v_0^{-1}v, \qquad g^* = (v_0 v_0)^{-1}g = \lambda_0/h_0\,. \tag{66}$$

In order to simplify the notation, the asterisks will be dropped henceforth, so all the quantities will be understood to be expressed in reduced units, unless stated otherwise.

The objective now is to find the solution to Eq. (62) as an expansion in powers of g:

$$f = f^{(0)} + f^{(1)}g + f^{(2)}g^2 + f^{(3)}g^3 + \cdots\,, \tag{67}$$

where $f^{(0)}$ is the equilibrium distribution function normalized to $p^{(0)} = 1$, $T^{(0)} = 1$. Similar expansions hold for the hydrodynamic fields

$$p = 1 + p^{(2)}g^2 + p^{(4)}g^4 + \cdots\,, \tag{68}$$

$$u_z = u^{(1)}g + u^{(3)}g^3 + \cdots\,, \tag{69}$$

$$T = 1 + T^{(2)}g^2 + T^{(4)}g^4 + \cdots\,, \tag{70}$$

where we have taken into account that, because of the symmetry of the problem, p and T are even functions of g, while u_z is an odd function. Insertion of Eq. (67) into Eq. (62) yields

$$(1 + \mathscr{A})f^{(n)} = f_{\mathrm{LE}}^{(n)} - \mathscr{D}f^{(n-1)} - \sum_{m=1}^{n-2} v^{(n-m)}(f^{(m)} - f_{\mathrm{LE}}^{(m)})\,, \tag{71}$$

where the operators $\mathscr{A}$ and $\mathscr{D}$ are defined as

$$\mathscr{A} \equiv v_r\frac{\partial}{\partial r} + \frac{v_\phi}{r}\left(v_\phi\frac{\partial}{\partial v_r} - v_r\frac{\partial}{\partial v_\phi}\right)\,, \tag{72}$$

$$\mathscr{D} \equiv \frac{\partial}{\partial v_z}\,. \tag{73}$$

The formal solution to Eq. (71) is

$$f^{(n)} = \sum_{k=0}^{\infty}(-\mathscr{A})^k\left[f_{\mathrm{LE}}^{(n)} - \mathscr{D}f^{(n-1)} - \sum_{m=1}^{n-2} v^{(n-m)}(f^{(m)} - f_{\mathrm{LE}}^{(m)})\right]\,. \tag{74}$$

This solution is not complete because $f^{(n)}$ appears implicitly on the right side through the dependence of $f_{\mathrm{LE}}^{(n)}$ on $p^{(n)}$, $u^{(n)}$ and $T^{(n)}$. If the space dependence of these quantities were known, Eq. (74) would give us $f^{(n)}$, provided that the previous contributions

$\{f^{(m)}, m \leqslant n-1\}$ are known. In order to get a closed set of equations for $p^{(n)}$, $u^{(n)}$ and $T^{(n)}$, we must apply the consistency conditions

$$\int d\mathbf{v}(f^{(n)} - f_{\mathrm{LE}}^{(n)}) = 0 , \tag{75}$$

$$\int d\mathbf{v}\, v_z(f^{(n)} - f_{\mathrm{LE}}^{(n)}) = 0 , \tag{76}$$

$$\int d\mathbf{v}\, v^2(f^{(n)} - f_{\mathrm{LE}}^{(n)}) = 0 . \tag{77}$$

4.1. First-order results

In this case, $f_{\mathrm{LE}}^{(1)} = -u^{(1)}\mathscr{D} f^{(0)}$, and so Eq. (74) yields

$$f^{(1)} = f_{\mathrm{LE}}^{(1)} - \mathscr{D}\left[f^{(0)} + \sum_{k=1}^{\infty}(-\mathscr{A})^k u^{(1)} f^{(0)}\right] , \tag{78}$$

where we have taken into account that the operators $\mathscr{A}$ and $\mathscr{D}$ commute and that $\mathscr{A}^k f^{(0)} = 0$ for $k \geqslant 1$. The conditions (75) and (77) are automatically satisfied. As for condition (76), it implies that

$$\int d\mathbf{v} \sum_{k=1}^{\infty}(-\mathscr{A})^k u^{(1)} f^{(0)} = -1 . \tag{79}$$

The simplest solution to Eq. (79) is expected to be of the form

$$u^{(1)}(r) = u_{12} r^2 . \tag{80}$$

To confirm this, let us express the operator $\mathscr{A}$ in Cartesian coordinates, i.e., $\mathscr{A} = v_x\partial/\partial x + v_y\partial/\partial y$. Consequently, only the terms with $k \leqslant 2$ contribute in Eqs. (78) and (79). Insertion of Eq. (80) into Eq. (79) then gives

$$u_{12} = -\tfrac{1}{4} . \tag{81}$$

The explicit expression for $f^{(1)}$ is simply

$$f^{(1)} = v_z\left[1 - \frac{1}{2}(v_r^2 + v_\phi^2) + \frac{1}{2} r v_r - \frac{1}{4} r^2\right] f^{(0)} . \tag{82}$$

The non-zero components of the pressure tensor and the heat flux are, to first order

$$P_{rz}^{(1)} = \int d\mathbf{v}\, v_r v_z f^{(1)} = \frac{1}{2} r , \tag{83}$$

$$q_z^{(1)} = \int d\mathbf{v}\left[\frac{1}{2} v^2 v_z f^{(1)} - u^{(1)}\left(v_z^2 + \frac{1}{2} v^2\right) f^{(0)}\right] = -1 . \tag{84}$$

4.2. Second-order results

The second-order contribution to the distribution function is

$$f^{(2)} = f_{\mathrm{LE}}^{(2)} - \mathscr{D} f^{(1)} + \sum_{k=1}^{\infty} (-\mathscr{A})^k (f_{\mathrm{LE}}^{(2)} - \mathscr{D} f^{(1)}) , \tag{85}$$

where

$$f_{\mathrm{LE}}^{(2)} = \left[\frac{1}{2} u^{(1)^2} (v_z^2 - 1) + p^{(2)} + \frac{1}{2} T^{(2)} (v^2 - 5) \right] f^{(0)} . \tag{86}$$

Eq. (76) is identically satisfied, since both $f_{\mathrm{LE}}^{(2)}$ and $\mathscr{D} f^{(1)}$ are even functions of v_z. Conditions (75) and (77) become, respectively,

$$\int \mathrm{d}\mathbf{v} \sum_{k=1}^{\infty} (-\mathscr{A})^k f_{\mathrm{LE}}^{(2)} = 0 , \tag{87}$$

$$\begin{aligned} \int \mathrm{d}\mathbf{v}\, v^2 \sum_{k=1}^{\infty} (-\mathscr{A})^k f_{\mathrm{LE}}^{(2)} &= -2 \int \mathrm{d}\mathbf{v}\, v_z (1 - \mathscr{A} + \mathscr{A}^2) f^{(1)} \\ &= 4 + \frac{1}{2} r^2 . \end{aligned} \tag{88}$$

Next, by looking for a solution with a spatial dependence similar to that of the planar case, Eqs. (52)–(54), we write

$$p^{(2)}(r) = p_{22} r^2 , \tag{89}$$

$$T^{(2)}(r) = T_{22} r^2 + T_{24} r^4 . \tag{90}$$

Consequently, only the terms with $k \leqslant 4$ contribute in Eqs. (87) and (88). More explicitly,

$$\begin{aligned} \sum_{k=1}^{\infty} (-\mathscr{A})^k f_{\mathrm{LE}}^{(2)} = \Bigg\{ & \left[p_{22} + \frac{T_{22}}{2} (v^2 - 5) \right] [- 2 r v_r + 2 (v_r^2 + v_\phi^2)] \\ & + \left[\frac{1}{32} (v_z^2 - 1) + \frac{T_{24}}{2} (v^2 - 5) \right] [- 4 r^3 v_r + 4 r^2 (3 v_r^2 + v_\phi^2) \\ & - 24 r v_r (v_r^2 + v_\phi^2) + 24 (v_r^2 + v_\phi^2)^2] \Bigg\} f^{(0)} . \end{aligned} \tag{91}$$

Insertion into Eqs. (87) and (88) yields

$$p_{22} + 48 T_{24} = 0 , \tag{92}$$

$$20 p_{22} + 20 T_{22} + 2688 T_{24} + 12 + (80 T_{24} + 1) r^2 = 4 + \frac{1}{2} r^2 \tag{93}$$

respectively. The solution is

$$p_{22} = \frac{3}{10}\,, \tag{94}$$

$$T_{22} = \frac{7}{50}, \quad T_{24} = -\frac{1}{160}\,. \tag{95}$$

The explicit expression for $f^{(2)}$ is then

$$\begin{aligned} f^{(2)} &= \sum_{k=0}^{4} (-\mathscr{A})^k f_{\mathrm{LE}}^{(2)} - \mathscr{D} \sum_{k=0}^{2} (-\mathscr{A})^k f^{(1)} \\ &= \left\{ (v_z^2 - 1)\left[1 - \frac{3}{2}(v_r^2 + v_\phi^2) + r v_r - \frac{1}{4} r^2\right] \right. \\ &\quad + \frac{1}{10}\left[3 + \frac{7}{10}(v^2 - 5)\right][2(v_r^2 + v_\phi^2) - 2 r v_r + r^2] \\ &\quad + \frac{1}{32}\left[v_z^2 - 1 - \frac{1}{10}(v^2 - 5)\right][24(v_r^2 + v_\phi^2)^2 - 24 r v_r (v_r^2 + v_\phi^2) \\ &\quad \left. + 4r^2(3v_r^2 + v_\phi^2) - 4r^3 v_r + r^4]\right\} f^{(0)}\,. \end{aligned} \tag{96}$$

The second-order contributions to the pressure tensor are

$$P_{rr}^{(2)} = \int \mathrm{d}\mathbf{v}\, v_r^2 f^{(2)} = -\frac{92}{25} + \frac{1}{20} r^2\,, \tag{97}$$

$$P_{\phi\phi}^{(2)} = \int \mathrm{d}\mathbf{v}\, v_\phi^2 f^{(2)} = -\frac{92}{25} + \frac{3}{20} r^2\,, \tag{98}$$

$$P_{zz}^{(2)} = \int \mathrm{d}\mathbf{v}\, v_z^2 f^{(2)} - u^{(1)^2} = \frac{184}{25} + \frac{7}{10} r^2\,. \tag{99}$$

Analogously,

$$q_r^{(2)} = \frac{1}{2} \int \mathrm{d}\mathbf{v}\, v^2 v_r f^{(2)} - u^{(1)} P_{rz}^{(1)} = \frac{1}{16} r^3\,. \tag{100}$$

4.3. Third- and fourth-order results

For $n = 3$, Eq. (74) reduces to

$$f^{(3)} = \sum_{k=0}^{\infty} (-\mathscr{A})^k [f_{\mathrm{LE}}^{(3)} - \mathscr{D} f^{(2)} - v^{(2)}(f^{(1)} - f_{\mathrm{LE}}^{(1)})]\,, \tag{101}$$

where

$$f_{\mathrm{LE}}^{(3)} = v_z \left[u^{(1)} f_{\mathrm{LE}}^{(2)} + \left(u^{(3)} - u^{(1)} T^{(2)} - \frac{1}{3} u^{(1)^3} v_z^2\right) f^{(0)}\right]\,. \tag{102}$$

Up to now, we have not needed to fix the temperature dependence of the collision frequency. This implies that to second order in the field the results are *universal*, i.e., independent of the interaction potential. On the other hand, the results of higher order are sensitive to the potential. For the sake of concreteness, we now consider repulsive interaction potentials of the form $\varphi(r) \propto r^{-\beta}$, for which the collision frequency is [21] $\nu \propto pT^{-(1-\alpha)}$ with $\alpha = \frac{1}{2} - 2/\beta$. In particular, the case $\alpha = 0$ corresponds to Maxwell molecules ($\beta = 4$), while the case $\alpha = \frac{1}{2}$ refers to hard spheres ($\beta \to \infty$). For this class of potentials, $\nu^{(2)} = p^{(2)} - (1-\alpha)T^{(2)}$.

Conditions (75) and (77) with $n = 3$ are identically satisfied because of symmetry. The structure of $u^{(1)}$, $p^{(2)}$ and $T^{(2)}$ suggests that $u^{(3)}$ has a spatial dependence of the form

$$u^{(3)}(r) = u_{32}r^2 + u_{34}r^4 + u_{36}r^6 \tag{103}$$

so only the terms with $k \leqslant 6$ contribute in Eq. (101). Insertion into Eq. (76) yields

$$34560u_{36} + 192u_{34} + 4u_{32} + \frac{2(1367 - 206\alpha)}{25} + \left(1728u_{36} + 16u_{34} + \frac{149 - 36\alpha}{50}\right) r^2 + \left(36u_{36} + \frac{4 - 3\alpha}{160}\right) r^4 = 0 \tag{104}$$

whose solution is

$$u_{32} = -\frac{4(100 - \alpha)}{25}, \quad u_{34} = -\frac{89 + 9\alpha}{800}, \quad u_{36} = -\frac{4 - 3\alpha}{5760}\,. \tag{105}$$

Once $u^{(3)}$ is determined, Eq. (101) gives the explicit form of $f^{(3)}$. From it we can easily get

$$P_{rz}^{(3)} = \int d\mathbf{v}\, v_r v_z f^{(3)} = \frac{1}{25}r^3 + \frac{1}{960}r^5\,, \tag{106}$$

$$q_z^{(3)} = \frac{1}{2}\int d\mathbf{v}\, v^2 v_z f^{(3)} - \frac{5}{2}u^{(3)} - u^{(1)}\left(\frac{3}{2}p^{(2)} + \frac{1}{2}u^{(1)^2} + P_{zz}^{(2)}\right) = \frac{4(1358 - 23\alpha)}{25} + \frac{209 - 3\alpha}{50}r^2 + \frac{15 - \alpha}{160}r^4\,. \tag{107}$$

Proceeding in a similar way, higher order terms can be evaluated, but the algebra becomes progressively more cumbersome. Here we only quote the main results to fourth order in g. Eq. (74) gives

$$f^{(4)} = \sum_{k=0}^{\infty} (-\mathscr{A})^k [f_{\mathrm{LE}}^{(4)} - \mathscr{D} f^{(3)} - \nu^{(2)}(f^{(2)} - f_{\mathrm{LE}}^{(2)})]\,. \tag{108}$$

By assuming that

$$p^{(4)}(r) = p_{42}r^2 + p_{44}r^4 + p_{46}r^6\,, \tag{109}$$

$$T^{(4)}(r) = T_{42}r^2 + T_{44}r^4 + T_{46}r^6 + T_{48}r^8 \tag{110}$$

it turns out that only the terms with $k \leqslant 8$ contribute in Eq. (108). By symmetry, condition (76) is identically satisfied. On the other hand, conditions (75) and (77) give, respectively

$$4p_{42} + 192p_{44} + 34560p_{46} + 192T_{44} + 69120T_{46} + 46448640T_{48} + \frac{8(243511 - 103801\alpha)}{625} + \left[\frac{14(95 - 56\alpha)}{25} + 16p_{44} + 1728p_{46} + 1728T_{46} + 1105920T_{48}\right] r^2 + \left[\frac{39(1-\alpha)}{200} + 36p_{46} + 6912T_{48}\right] r^4 = 0\,, \tag{111}$$

$$\frac{4(448099 - 1773928\alpha)}{625} + 20T_{42} + 1728T_{44} + 546048T_{46} + 403881984T_{48} - \left[\frac{134783 - 59955\alpha}{250} + 80T_{44} + 15552T_{46} + 8736768T_{48}\right] r^2 + \left[\frac{1345 - 642\alpha}{400} + 180T_{46} + 62208T_{48}\right] r^4 + \left[\frac{11 - 9\alpha}{960} + 320T_{48}\right] r^6 = 0\,, \tag{112}$$

where in Eq. (112) we have eliminated p_{42}–p_{46} in favor of $T_{42} - T_{48}$. The solution to Eqs. (111) and (112) is

$$p_{42} = -\frac{218083 - 11035\alpha}{1250}, \quad p_{44} = -\frac{653 - 176\alpha}{2000}, \quad p_{46} = \frac{7 - \alpha}{4800}\,, \tag{113}$$

$$T_{42} = -\frac{2501129 - 38495\alpha}{6250}, \quad T_{44} = -\frac{32057 - 663\alpha}{20000}\,,$$
$$T_{46} = -\frac{454 + 87\alpha}{72000}, \quad T_{48} = -\frac{11 - 9\alpha}{307200}\,. \tag{114}$$

From Eq. (108) we can now evaluate the fourth-order terms in the pressure tensor and the heat flux. The results are

$$P_{rr}^{(4)} = \int d\mathbf{v}\, v_r^2 f^{(4)} = \frac{4(5087846 - 175355\alpha)}{3125} - \frac{106029 - 3653\alpha}{2500} r^2 - \frac{287 - 18\alpha}{6000} r^4 + \frac{3 - \alpha}{19200} r^6\,, \tag{115}$$

$$P_{\phi\phi}^{(4)} = \int d\mathbf{v}\, v_\phi^2 f^{(4)} = \frac{4(5087846 - 175355\alpha)}{3125} - \frac{3(106029 - 3653\alpha)}{2500} r^2 - \frac{287 - 18\alpha}{1200} r^4 + \frac{7(3 - \alpha)}{19200} r^6\,, \tag{116}$$

$$P_{zz}^{(4)} = \int d\mathbf{v}\, v_z^2 f^{(4)} - 2u^{(1)}u^{(3)} - u^{(1)^2}(p^{(2)} - T^{(2)})$$

$$= -\frac{8(5087846 - 175355\alpha)}{3125} - \frac{442191 - 25799\alpha}{1250} r^2$$

$$- \frac{1385 - 492\alpha}{2000} r^4 + \frac{15 - \alpha}{4800} r^6 , \tag{117}$$

$$q_r^{(4)} = \frac{1}{2} \int d\mathbf{v}\, v^2 v_r f^{(4)} - u^{(1)} P_{rz}^{(3)} - u^{(3)} P_{rz}^{(1)}$$

$$= \frac{100 - \alpha}{25} r^3 + \frac{97 + 9\alpha}{2400} r^5 + \frac{5 - 3\alpha}{15360} r^7 . \tag{118}$$

It can be checked that the results for $p(r)$, $T(r)$, $u_z(r)$, $P_{rr}(r)$, $P_{\phi\phi}(r)$, $P_{r\phi}(r)$ and $q_r(r)$ we have derived are indeed consistent with the balance equations (25)–(27). In fact, Eq. (26) allows us to obtain $P_{rz}^{(5)}(r)$ with the result

$$P_{rz}^{(5)} = \frac{3(235119 + 2780\alpha)}{12500} r^3 + \frac{25079 + 1097\alpha}{120000} r^5$$

$$+ \frac{71 + 9\alpha}{72000} r^7 + \frac{23 - 9\alpha}{3072000} r^9 . \tag{119}$$

5. Discussion

When Eqs. (80), (81), (89), (90), (94), (95), (103), (105), (109), (110), (113) and (114) are inserted into Eqs. (68)–(70), one gets the hydrodynamic profiles predicted by the BGK kinetic model through fourth order in the field. Comparison with the NS predictions, Eqs. (38)–(40), indicates that the latter, while providing the correct values of u_{12}, u_{36}, T_{24} and T_{48}, do not capture the pressure variation ($p_{22}^{\mathrm{NS}} = p_{42}^{\mathrm{NS}} = p_{44}^{\mathrm{NS}} = p_{46}^{\mathrm{NS}} = 0$) or the lower-degree terms of the velocity ($u_{32}^{\mathrm{NS}} = u_{34}^{\mathrm{NS}} = 0$) and temperature ($T_{22}^{\mathrm{NS}} = T_{42}^{\mathrm{NS}} = T_{44}^{\mathrm{NS}} = T_{46}^{\mathrm{NS}} = 0$) profiles.

The results derived in the previous Section strongly support the conjecture that the expansion in powers of g is asymptotic rather than convergent [9]. For instance $T = 1 + 0.14g^2 - 4.0 \times 10^2 g^4 + \cdots$ and $T = 1 - 0.41g^2 - 1.1 \times 10^4 g^4 + \cdots$ at $r = 1$ and $r = 5$, respectively. Thus, the expansion is only useful if g is small enough to keep the first few terms only. As we did in the planar case, Section 3, we now give the hydrodynamic profiles through third order in real units:

$$p(r) = p_0 \left[1 + \zeta_p \left(\frac{mg}{k_B T_0} \right)^2 r^2 \right] + \mathcal{O}(g^4) , \tag{120}$$

$$u_z(r) = u_0 - \frac{\rho_0 g}{4\eta_0} r^2 \left[1 + \frac{(4 - 3\alpha)\rho_0^2 g^2}{576\eta_0\kappa_0 T_0} r^4 + \zeta_u \left(\frac{mg}{k_B T_0} \right)^2 r^2 + \zeta_u' \frac{\rho_0 \eta_0^2 g^2}{p_0^3} \right] + \mathcal{O}(g^5), \tag{121}$$

$$T(r) = T_0 \left[1 - \frac{\rho_0^2 g^2}{64\eta_0\kappa_0 T_0} r^4 + \zeta_T \left(\frac{mg}{k_B T_0} \right)^2 r^2 \right] + \mathcal{O}(g^4) , \tag{122}$$

where $\zeta_p = \frac{3}{10}$, $\zeta_u = (89 + 9\alpha)/200$, $\zeta_u' = \frac{16}{25}(100 - \alpha)$ and $\zeta_T = \frac{7}{50}$. The structure of these profiles is similar to that of the planar case, Eqs. (52)–(54). In particular, the temperature presents a local minimum at $r = 0$ and a maximum at $r = \sqrt{32\zeta_T}\ell_0 \equiv r_{\max}$, where $\ell_0 \equiv (\eta_0\kappa_0 T_0)^{1/2}/p_0$. The relative difference between the maximum and the minimum is $(T_{\max} - T_0)/T_0 = 16\zeta_T^2(\ell_0/h_0)^2$, where $h_0 \equiv (k_B T_0/m)/g$. The distance from the center of the points where the temperature reaches the value $T_{\max}$ in the pipe flow ($r_{\max} \simeq 2.12\ell_0$) is very close to that of the channel flow ($y_{\max} \simeq \pm 2.14\ell_0$). On the other hand, the effect is considerably smaller in the former case [$(T_{\max} - T_0)/T_0 \simeq 0.31(\ell_0/h_0)^2$] than in the latter [$(T_{\max} - T_0)/T_0 \simeq 1.7(\ell_0/h_0)^2$]. The equation of state is also similar to that of the planar case, Eq. (55),

$$T = T_0 - \frac{\eta_0}{4\kappa_0}(u_0 - u_z)^2 + \frac{\zeta_T}{\zeta_p}\frac{T_0}{p_0}(p - p_0) + \mathcal{O}(g^4) . \tag{123}$$

As for the momentum and heat fluxes, the results through third order are

$$P_{rr}(r) = p_0 \left[1 - \frac{92}{25}\frac{\rho_0\eta_0^2 g^2}{p_0^3} + \frac{1}{20}\left(\frac{mg}{k_B T_0} \right)^2 r^2 \right] + \mathcal{O}(g^4) , \tag{124}$$

$$P_{\phi\phi}(r) = p_0 \left[1 - \frac{92}{25}\frac{\rho_0\eta_0^2 g^2}{p_0^3} + \frac{3}{20}\left(\frac{mg}{k_B T_0} \right)^2 r^2 \right] + \mathcal{O}(g^4) , \tag{125}$$

$$P_{zz}(r) = p_0 \left[1 + \frac{184}{25}\frac{\rho_0\eta_0^2 g^2}{p_0^3} + \frac{7}{10}\left(\frac{mg}{k_B T_0} \right)^2 r^2 \right] + \mathcal{O}(g^4) , \tag{126}$$

$$P_{rz}(r) = \frac{\rho_0 g}{2} r \left[1 + \frac{\rho_0^2 g^2}{192\eta_0\kappa_0 T_0} r^4 + \frac{2}{25}\left(\frac{mg}{k_B T_0} \right)^2 r^2 \right] + \mathcal{O}(g^5) , \tag{127}$$

$$q_r(r) = \frac{\rho_0^2 g^2}{16\eta_0} r^3 + \mathcal{O}(g^4) , \tag{128}$$

$$q_z(r) = -\frac{2mg\kappa_0}{5k_B} \left[1 - \frac{4(1358 - 23\alpha)\rho_0\eta_0^2 g^2}{25 p_0^3} - \frac{209 - 3\alpha}{50}\left(\frac{mg}{k_B T_0} \right)^2 r^2 - \frac{(15 - \alpha)\rho_0^2 g^2}{64\eta_0\kappa_0 T_0} r^4 \right] + \mathcal{O}(g^5) . \tag{129}$$

As expected, they strongly differ from the NS results, Eqs. (31), (34), (41) and (42), with the exception of q_r, in which case the error of the NS value is of order g^4.

The non-monotonic behavior of $T(r)$ is not only an interesting effect but also a counterintuitive result, given that the radial component of the heat flux monotonically increases with the distance from the pipe axis. Consider the inner cylinder $r \leqslant r_{\max}$.

Within that region the temperature increases radially and yet the heat flows outwards from the colder to the hotter points! The solution to this paradox lies in the dramatic breakdown of the Fourier law (33) within the region $r \leqslant r_{\max}$. Following Hess and Malek Mansour [15], a heuristic extension of the Fourier law can be written as

$$-\kappa \frac{\partial T}{\partial r} = q_r - \xi^2 \nabla^2 q_r \,, \tag{130}$$

where ξ is a characteristic distance of the order of the mean free path. According to Eq. (130), the sign of the thermal gradient results from the competition between q_r and its Laplacian. The simple estimate $\nabla^2 q_r = r^{-1}\partial(r\partial q_r/\partial r)/\partial r \sim q_r/r^2$ shows that $\partial T/\partial r > 0$ for $r < \xi$. It is easy to check that Eq. (130), with $\xi = \frac{1}{3} r_{\max} \simeq 0.71 \ell_0$, is indeed consistent with the profiles (122) and (128). If one characterizes the deviation from the Fourier law by means of an *apparent* thermal conductivity coefficient defined by

$$q_r = -\kappa_{\rm app} \frac{\partial T}{\partial r} \tag{131}$$

then one has

$$\frac{\kappa_{\rm app}}{\kappa} = \left[1 - \left(\frac{r_{\max}}{r}\right)^2\right]^{-1} + \mathcal{O}(g^2) \,. \tag{132}$$

The above ratio vanishes at $r = 0$, is negative in the interval $0 < r < r_{\max}$, diverges at $r = r_{\max}$, and finally tends to unity from above for $r \gg r_{\max}$.

The breakdown of the Newton law is characterized by an apparent shear viscosity coefficient defined by

$$P_{rz} = -\eta_{\rm app} \frac{\partial u_z}{\partial r} \,. \tag{133}$$

The ratio between this coefficients and the NS shear viscosity is

$$\begin{aligned} \frac{\eta_{\rm app}}{\eta} &= 1 - \zeta_u' \frac{\rho_0^2 g^2}{p_0^3} - \frac{19-\alpha}{20} \left(\frac{mg}{k_B T_0}\right)^2 r^2 + \mathcal{O}(g^4) \\ &= 1 - \frac{\zeta_u'}{5\zeta_T} \frac{\ell_0^2}{T_0} \frac{\partial^2 T}{\partial r^2} - \frac{2(2533-31\alpha)}{175} \frac{\ell_0^2}{v_0^2} \left(\frac{\partial u_z}{\partial r}\right)^2 + \mathcal{O}(g^4) \,. \end{aligned} \tag{134}$$

The last line of Eq. (134) clearly shows that $\eta_{\rm app}$ incorporates super-Burnett terms. Those terms can be written in equivalent alternative forms by taking into account that

$$\frac{\partial^2 T}{\partial r^2} = -\frac{3\eta_0}{4\kappa_0} \left(\frac{\partial u_z}{\partial r}\right)^2 + \frac{\zeta_T}{\zeta_p} \frac{T_0}{p_0} \frac{\partial^2 p}{\partial r^2} + \mathcal{O}(g^4) \,. \tag{135}$$

As an illustration of the corrections over the NS description provided by kinetic theory, we compare in Figs. 1–3 the hydrodynamic and flux profiles for the case $g = 0.1 v_0 (k_B T_0/m)^{1/2}$ [which corresponds to $(h_0/\ell_0)^2 = 40$], as predicted by both descriptions when only terms through third order in g are retained. Although higher order

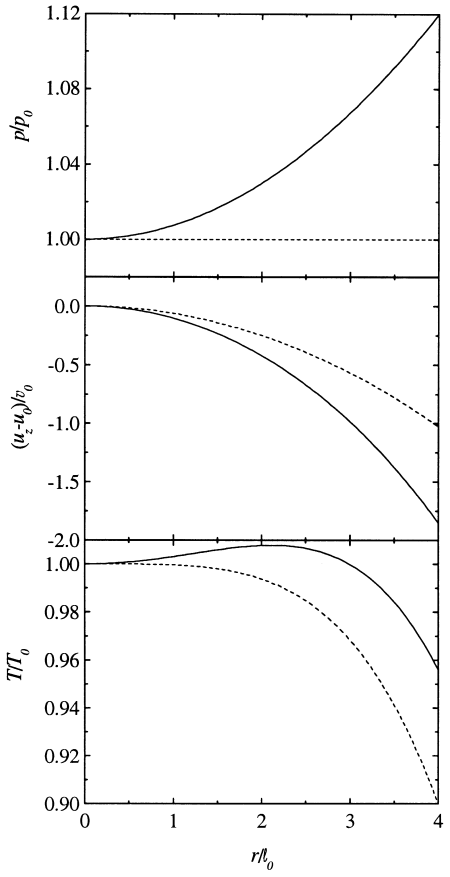

Fig. 1. Hydrodynamic profiles for the case $g=0.1v_0v_0$, as predicted by the Navier–Stokes description (dashed lines) and by the kinetic theory description (solid lines).

terms are not necessarily negligible for that particular value of the field, the retained terms can be expected to be enough, at least at a qualitative level. The curves for u_z and q_z correspond to hard spheres ($\alpha = \frac{1}{2}$), but they are practically indistinguishable from those of Maxwell molecules ($\alpha = 0$). Except for the shear stress P_{rz} and the radial heat flux q_r, the kinetic theory predictions dramatically differ from the NS ones. The hydrostatic pressure grows quadratically rather than being uniform, the flow velocity decreases more rapidly than expected from the NS description, and the temperature exhibits a non-monotonic behavior. Normal stress differences appear, the flux of longitudinal momentum along the longitudinal direction being larger than the other two normal stresses ($P_{zz} > P_{\phi\phi} > P_{rr}$). Finally, the longitudinal heat flux is not only different from zero (despite the absence of longitudinal gradients), but it can be even larger than the radial heat flux. These features are qualitatively similar to those found in the rectangular geometry (cf. Section 3), which have been confirmed by computer simulations [10,13,14].

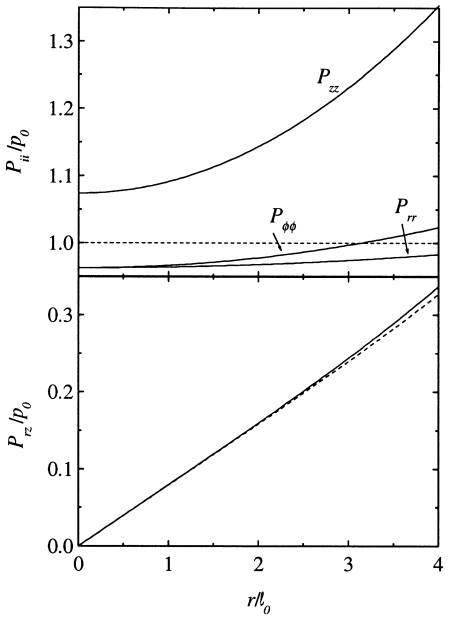

Fig. 2. Same as in Fig. 1 but for the elements of the pressure tensor.

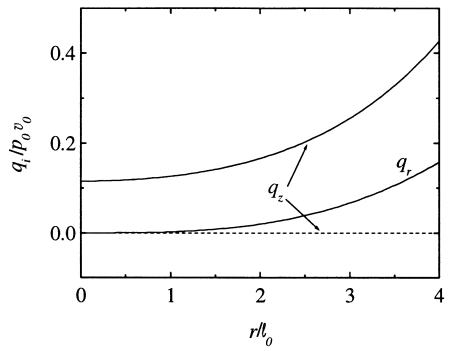

Fig. 3. Same as in Fig. 1 but for the components of the heat flux.

6. Conclusions

In this paper we have solved the BGK kinetic equation for the (laminar) steady *cylindrical* Poiseuille flow fed by a constant gravity field. The solution has been obtained as a perturbation expansion in powers of the field through fourth order and for a general class of repulsive potentials. The results exhibit a very weak sensitivity to the interaction potential and strongly indicate that the expansion is only asymptotic. A comparison with the profiles obtained from the Navier–Stokes (NS) constitutive equations shows that the latter widely fail over distances comparable to the mean free

path. At a qualitative level, the most important limitation of the NS description is that it predicts a monotonically decreasing temperature as one moves apart from the cylinder axis. In contrast, the kinetic theory description shows that the temperature has a local minimum ($T = T_0$) at the axis ($r = 0$) and reaches a maximum value ($T = T_{\max}$) at a distance from the center ($r = r_{\max}$) of the order of the mean free path. In the region $r \leqslant r_{\max}$, the radial heat flows from the colder to the hotter points, what dramatically illustrates the breakdown of the Fourier law. Furthermore, a longitudinal component of the heat flux exists in the absence of gradients along the longitudinal direction. Non-Newtonian effects are exemplified by the non-uniformity of the hydrostatic pressure and by the presence of normal stress differences.

The above effects are similar to those previously found in the case of a rectangular channel. This is a non-trivial result, since both geometries are quite different, as can be expected from the different mathematical structure of the balance equations [Eqs. (1)–(3) versus Eqs. (25)–(27)] and of the kinetic equations [Eq. (51) versus Eq. (62)]. In the rectangular geometry the relevant space variable y takes both positive and negative values, while the radial variable r is positive definite. Also, the normal stress along the gradient direction is uniform in the rectangular case ($P_{yy} = \text{const}$) and non-uniform in the cylindrical case ($P_{rr} \neq \text{const}$). At a quantitative level, on the other hand, the deviations of the NS profiles from the kinetic theory ones are weaker in the cylindrical geometry than in the rectangular geometry. For instance, the relative difference $(T_{\max} - T_0)/T_0$ is about 5 times smaller in the former case than in the latter.

The analysis carried out in this work can be extended to the Boltzmann equation for Maxwell molecules, as already done in the channel case [12]. The hydrodynamic profiles will still be given by Eqs. (120)–(122), but with different numerical values for the coefficients ζ_p, ζ_u, ζ_u' and ζ_T. For hard spheres, the solution can be obtained by approximate schemes, such as the moment method [15]. Finally, we hope that the results reported in this paper may stimulate the undertaking of computer simulations of the Poiseuille flow induced by gravity in a pipe.

Acknowledgements

This work has been done under the auspices of the Agencia Española de Cooperación Internacional (Programa de Cooperación Interuniversitaria Hispano-Marroquí). A.S. acknowledges partial support from the DGES (Spain) through Grant No. PB97-1501 and from the Junta de Extremadura (Fondo Social Europeo) through Grant No. IPR99C031.

References

[1] D.J. Tritton, Physical Fluid Dynamics, Oxford University Press, Oxford, 1988.
[2] G.K. Batchelor, An Introduction to Fluid Dynamics, Cambridge University Press, Cambridge, 1967.
[3] R.B. Bird, W.E. Stewart, E.W. Lightfoot, Transport Phenomena, Wiley, New York, 1960.

[4] H. Lamb, Hydrodynamics, Dover, New York, 1945.
[5] L.P. Kadanoff, G.R. McNamara, G. Zanetti, Complex Syst. 1 (1987) 791.
[6] L.P. Kadanoff, G.R. McNamara, G. Zanetti, Phys. Rev. A 40 (1989) 4527.
[7] M. Alaoui, A. Santos, Phys. Fluids A 4 (1992) 1273.
[8] R. Esposito, J.L. Lebowitz, R. Marra, Commun. Math. Phys. 160 (1994) 49.
[9] M. Tij, A. Santos, J. Stat. Phys. 76 (1994) 1399. Note a misprint in Eq. (59): the denominators 25, 30, 3125, 750 and 250 should be multiplied by 3, 5, 3, 5 and 7, respectively.
[10] M. Malek Mansour, F. Baras, A.L. Garcia, Physica A 240 (1997) 255.
[11] K.P. Travis, B.D. Todd, D.J. Evans, Physica A 240 (1997) 315.
[12] M. Tij, M. Sabbane, A. Santos, Phys. Fluids 10 (1998) 1021.
[13] D. Risso, P. Cordero, Phys. Rev. E 58 (1998) 546.
[14] F.J. Uribe, A.L. Garcia, Phys. Rev. E 60 (1999) 4063.
[15] S. Hess, M. Malek Mansour, Physica A 272 (1999) 481.
[16] U. Frisch, B. Hasslacher, Y. Pomeau, Phys. Rev. Lett. 56 (1986) 1505.
[17] E.S. Asmolov, N.K. Makashev, V.I. Nosik, Dokl. Akad. Nauk SSSR 249 (1979) 577 (Sov. Phys. Dokl. 24 (1979) 892).
[18] A. Santos, V. Garzó, in: J. Harvey, G. Lord (Eds.), Rarefied Gas Dynamics, Oxford University Press, Oxford, 1995, pp. 13–22.
[19] S. Chapman, T.G. Cowling, The Mathematical Theory of Nonuniform Gases, Cambridge University Press, Cambridge, 1970.
[20] J.M. Montanero, A. Santos, V. Garzó, Phys. Fluids (in press) and preprint cond-mat/0003364.
[21] C. Cercignani, The Boltzmann Equation and Its Applications, Springer, New York, 1988.
[22] J.V. Iribarne, H.-R. Cho, Atmospheric Physics, Kluwer, Dordrecht, 1980.
[23] J.W. Chamberlain, Theory of Planetary Atmospheres. An Introduction to Their Physics and Chemistry, Academic Press, New York, 1978.